IJST, Transactions of Civil Engineering, Vol. 39, No. C2+, pp 469-483
Printed in The Islamic Republic of Iran, 2015

A PRACTICAL PROCEDURE TO ESTIMATE THE BEARING CAPACITY OF FOOTINGS ON SAND–APPLICATION TO 87 CASE STUDIES*

M. VEISKARAMI[1**], J. KUMAR[2] AND F. VALIKHAH[3]

[1]University of Guilan, also Shiraz University, I. R. of Iran
Email: mveiskarami@gmail.com
[2]Dept. of Civil Engineering, Indian Institute of Science, Bangalore – 560012, India
[3]University of Guilan, also Amir Kabir University of Technology, I. R. of Iran

Abstract– Following the recent work of the authors in development and numerical verification of a new kinematic approach of the limit analysis for surface footings on non-associative materials, a practical procedure is proposed to utilize the theory. It is known that both the peak friction angle and dilation angle depend on the sand density as well as the stress level, which was not the concern of the former work. In the current work, a practical procedure is established to provide a better estimate of the bearing capacity of surface footings on sand which is often non-associative. This practical procedure is based on the results obtained theoretically and requires the density index and the critical state friction angle of the sand. The proposed practical procedure is a simple iterative computational procedure which relates the density index of the sand, stress level, dilation angle, peak friction angle and eventually the bearing capacity. The procedure is described and verified among available footing load test data.

Keywords– Foundation, sand, non-associated flow rule, limit analysis, stress characteristics

1. INTRODUCTION

Practical interpretation of the "bearing capacity" is often questionable [1, 2] and there are a number of analytical and numerical methods to estimate the bearing capacity. The research dates back to the early 1920s [3, 4] which later resulted in the popular bearing capacity equation of Terzaghi [5] with three different bearing capacity factors. It was subjected to some modifications during the 1950s to 1970s [6-9]. Owing to Sokolovskii [10], a rigorous theoretical framework, based on the method of stress characteristics, was established to solve different stability problems in soil mechanics. Based on this theory and the limit theorems developed by Drucker and Prager [11], a number of studies were made based on the upper bound and lower bound theorems of the limit analysis in conjunction with the finite elements and linear/nonlinear programming [12]. The method of stress characteristics for finding the bearing capacity of shallow foundations has been applied by a number of researchers [13-16]. In recent years, the influence of several other factors has also attracted special attention, for example: (i) the bearing capacity of unsaturated soils [17], (ii) the effect of base roughness [18], and (iii) scale and stress level effects [19-22]. While there are a number of studies on the theoretical estimation of the bearing capacity for an associated flow rule material, only limited investigations are available where the effect of non-associativity has been considered [23-27].

Most frictional soils, in particular sands, are non-associative materials [28]. Bolton [28] showed that the non-associativity can be related to soil packing, through the density index, and the stress level. On the

*Received by the editors April 23, 2014; Accepted May 23, 2015.
**Corresponding author

other hand, the stress level plays a very important role on mobilization of the friction angle. Attempts made by both Meyerhof [29] and De Beer [30], who considered the effect of stress level on the mobilized soil friction angle along the failure path beneath surface footings, reveal that the magnitudes of the bearing capacity factors depend on size of the footing.

Very recently, the authors [27] examined the influence of non-associativity of soil on the bearing capacity, and developed a new kinematic approach of the upper bound limit analysis for non-associated materials. In this approach, the failure mechanism was no longer assumed; in contrast, it was established by using the method of stress characteristics. The proposed approach was used to develop some design charts for the third bearing capacity factor, N_γ.A practical procedure is presented and described in the current paper to verify the theoretical results with a rather large number of available test results and to provide an effective procedure to apply the method for practical purposes. This is an iterative procedure based on soil critical state friction angle and the density index which are often used to characterize sands. The angle of dilation is known to depend on the density index of the sand and the mean stress [28] whereas the mean stress has been related to the ultimate footing pressure [30]. It is worth mentioning that since surface footings on sand are studied, only the third bearing capacity factor, N_γ, is focused. This paper presents a brief review of the proposed approach and then explains the practical procedure and verifications.

2. BRIEF REVIEW OF THE PROPOSED APPROACH

As stated earlier, the current work is mainly based on the results of a recently developed methodology (a proposed approach) by the authors [27]. In this new approach, the failure mechanism is no longer assumed *a priori*, as it is common in most kinematic approaches of the upper bound limit analysis. The failure mechanism is first determined by the method of stress characteristics which seems to be valid as stress characteristics field coincides with those regions experiencing plastic deformation. Therefore, slip lines define the failure pattern beneath a footing. On the other hand, the internal energy dissipation of non-associative materials obeying the Mohr-Coulomb failure criterion requires the tractions to be known on velocity discontinuities. In the proposed approach it is assumed that the normal component of the traction vector remains constant along slip lines and hence, since the tractions along slip lines are known, the internal energy dissipation can be computed for both associative and non-associative materials. This assumption was found to be quite reasonable as the stress field and the solution obtained by the method of stress characteristics is close to the upper bound limit [31]. Therefore, the proposed approach comprises two distinct elements: (i) the stress field and the failure mechanism from the method of stress characteristics and (ii) the velocity field and the work (energy rate) equations from the kinematic approach of the upper bound limit analysis.

a) The stress field by the method of stress characteristics

The method of stress characteristics, developed in the 1960's, is a well-known method for solving stability problems in soil mechanics which combines the equilibrium and yield equations along two families of the stress characteristics. Details on this method can be found in the literature [10, 32, 33; among many]. First, the equilibrium equations are:

$$\begin{cases} \frac{\partial \sigma_{xx}}{\partial x} + \frac{\partial \tau_{xz}}{\partial z} = X \\ \frac{\partial \sigma_{zz}}{\partial z} + \frac{\partial \tau_{xz}}{\partial x} = Z \end{cases} \quad (1)$$

where, σ_{xx}, $\sigma_{zz}$and τ_{xz} are the components of stresses, X and Z are body forces per unit volume in x and z directions, respectively. By defining the angle θbetween the major principal stress direction and horizontal direction and the mean stress, $\sigma = (\sigma_{xx} + \sigma_{zz})/2$ and implementation of the Mohr-Coulomb yield criterion, it is possible to find all components of stress at a point as [34, 32]:

$$\sigma_{xx} = \sigma(1 + \sin\phi\cos 2\theta) + c\cos\phi\cos 2\theta \quad (2a)$$

$$\sigma_{zz} = \sigma(1 - \sin\phi\cos 2\theta) + c\cos\phi\cos 2\theta \quad (2b)$$

$$\tau_{xz} = \sigma\sin\phi\sin 2\theta + c\cos\phi\sin 2\theta \quad (2c)$$

The two stress characteristics directions are defined by using the equations:

$$\frac{dz}{dx} = \tan(\theta \pm \mu) \quad (3)$$

where $\mu = \frac{\pi}{4} - \frac{\phi}{2}$; and$c$ and ϕ are soil shear strength parameters. Therefore, the governing equations along the two families of stress characteristics are as follows:

$$\sigma \pm 2(\sigma tan\phi + c)d\theta = \mp X(tan\phi dz \mp dx) \pm Z(tan\phi dx \pm dz) \quad (4)$$

b) The velocity field and the upper bound limit analysis

Assuming that the shear planes coincide with the characteristics of stress, the kinematic approach of the upper bound limit analysis can be used for both associative and non-associative materials. The energy rate balance equation can then be used to find an upper bound estimate of the limit load. The energy rate balance equation is as follows:

$$\int_S \boldsymbol{t}.\dot{\boldsymbol{v}}^{\boldsymbol{p}} dA + \int_V \boldsymbol{b}.\dot{\boldsymbol{v}}^{\boldsymbol{p}} dV \leq \int_V \boldsymbol{\sigma}:\dot{\boldsymbol{\varepsilon}}^{\boldsymbol{p}} dV \quad (5)$$

where $\boldsymbol{t}$is the surface traction, $\dot{\boldsymbol{v}}^{\boldsymbol{p}}$is the rate of plastic displacements (velocity increment), S is the surface boundary, $\boldsymbol{b}$is thebody forcevector per unit volume, $\boldsymbol{\sigma}$is the stress tensor, $\dot{\boldsymbol{\varepsilon}}^{\boldsymbol{p}}$is the rate of plastic strain tensor and V is the volume. In the conventional method, a compatible failure mechanism is assumed and it is optimized to find the minimum upper bound load.

c) The proposed approach of the upper bound limit analysis

In the proposed approach, the failure mechanism is found by nature when the method of stress characteristics is applied [27]. To explain how the proposed approach works, consider a typical stress characteristics network constructed for some arbitrary problem. This is shown typically in Fig. 1a for a smooth base footing. On the same figure, a cinematically admissible velocity field is constructed (only velocity vectors along the lowermost failure plane are shown) based on a velocity hodograph. Figure 1b, shows a typical element having its four edges sliding on shear planes or velocity discontinuities. The absolute velocity of this block is $\vec{v}_a$and the resultant of body forces acting on this block is $\vec{b}$.The velocity discontinuity for the lowermost boundary of this block is typically shown in Fig. 1c,on which, the traction vector, $\vec{T}$, is shown and decomposed into the normal and the shear components. Assume that the volume dilation along the shear plane takes place at an arbitrary angle, ψ (dilation angle). In associative materials, $\psi = \phi$ whereas in non-associative materials, $\psi < \phi$.

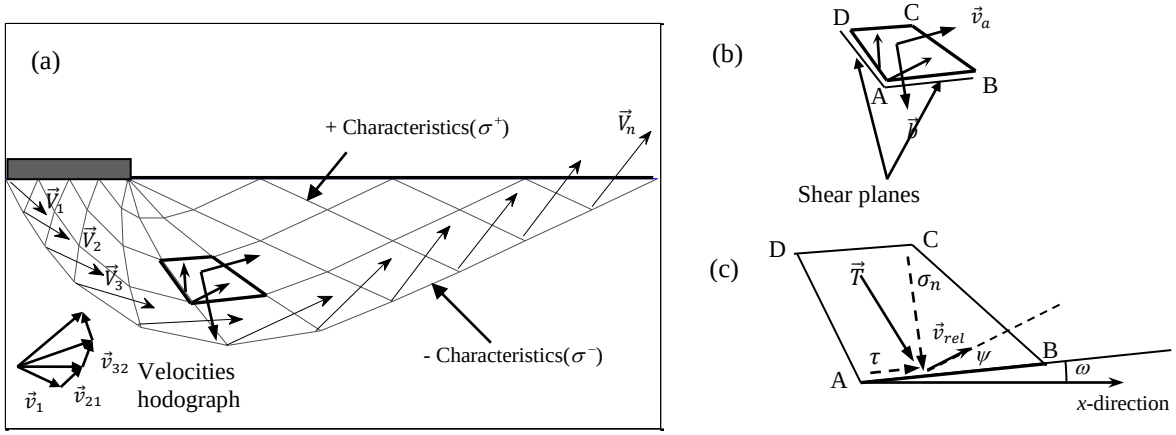

Fig. 1. Schematic representation of the failure mechanism established based on the stress characteristics net: (a) the stress characteristics net, (b) a typical element enclosed by four shear planes and (c) traction vector on a shear plane and an arbitrary plastic shearing

The energy balance equation can now be applied to all these blocks to compute both the rate of the external work (done by body forces) and the rate of the internal energy dissipation (at velocity discontinuities). Finally, the total rate of external works and energy dissipation can be calculated by summing up these values computed for all individual blocks. For an arbitrary block these two rates can be calculated as follows:

$$\dot{W}_{ext} = \vec{v}_a . \vec{b} \tag{6a}$$

$$\dot{E}_{int} = \vec{T} . \vec{v}_{rel} L_{AB} = \sigma_n L_{AB} v_{rel} \sin\psi + \tau L_{AB} v_{rel} \cos\psi \tag{6b}$$

In these equations, $\dot{W}_{ext}$is the rate of external work, $\dot{E}_{int}$ is the rate of internal energy dissipation, $\vec{v}_a$ is the absolute velocity of the rigid block, $\vec{b}$is the body force applied on the rigid block, $\vec{T}$is the traction vector acting on a velocity discontinuity, $\vec{v}_{rel}$is the relative velocity of two neighboring blocks, σ_n and τ ($= \sigma_n \tan\phi$) are normal and shear components of the traction vector, $L_{AB}$is the length of a discontinuity boundary (here, AB) and ψ is the angle of dilation. It is important to note that for associative materials, where $\psi = \phi$, the rate of internal energy dissipation given by this equation becomes zero. For non-associative materials, the traction vector acting on the velocity discontinuity plane is required. The normal component of the traction vector, σ_n, by using Eq. (2b) can be found as follows:

$$\sigma_n = \sigma(1 - \sin\phi \cos 2(\theta - \omega)) + c \cos\phi \cos 2(\theta - \omega) \tag{7}$$

where, $\omega$is the angle between the plane of velocity discontinuity and the horizontal direction. The computational procedure is performed over all rigid blocks and for the footing itself. Details of the procedure can be found in Veiskarami *et al.* (2014) [27].

Based on the proposed approach, a number of analyses were made to find the variations of the bearing capacity factor, N_γ against the dilation and friction angle. Figure 2 shows the bearing capacity factor, N_γ, versus soil friction angle with different flow rules[27]. With very good accuracy, a simple curve-fitting suggests the following equation to represent these design charts which are helpful for practical applications and for computer programming where interpolations between consecutive curves are required. Parameters α and $\beta$are given in Table 1 corresponding to ψ/ϕ ratio and footing roughness.

$$N_\gamma = \alpha e^{\beta\phi} \tag{8}$$

Table 1. Parameters α and β used to approximate the design charts for N_γ

ψ/ϕ	Smooth Base		Rough Base	
	α	β	α	β
0	0.088	0.131	0.586	0.111
0.25	0.069	0.145	0.452	0.125
0.50	0.054	0.159	0.344	0.139
0.75	0.042	0.170	0.270	0.151
1.00	0.036	0.178	0.241	0.157

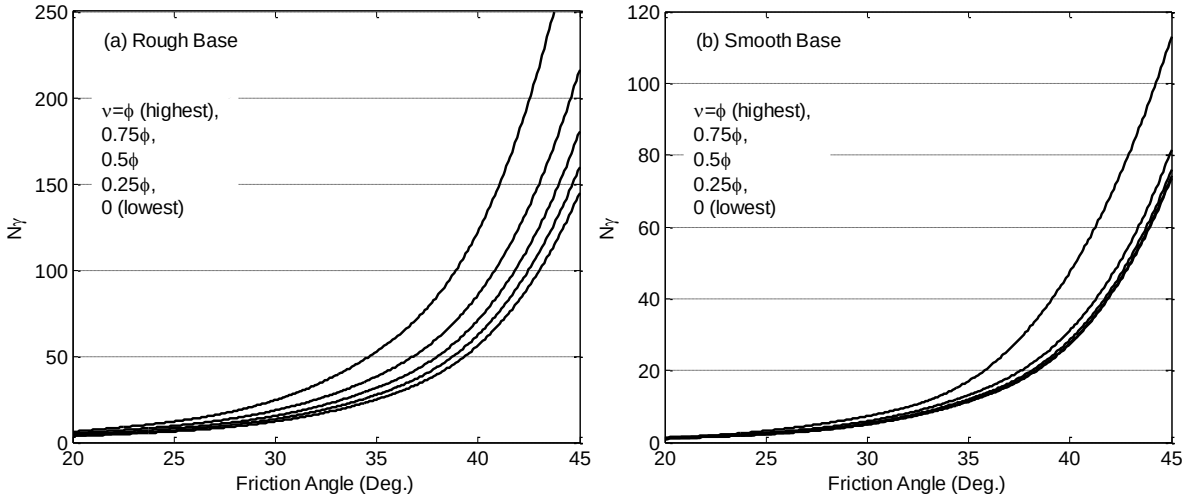

Fig. 2. Bearing capacity factor, N_γ, with the proposed method for both (a) rough base and (b) smooth base strip foundations

The proposed approach requires the angle of dilation to be known. In sand, a comprehensive study by Bolton [28] indicated that the angle of dilation depends on the packing (often quantified by the density index, D_r) and the stress level. In the practical procedure, these two issues are utilized to effectively apply the proposed approach of the upper bound limit analysis for non-associative materials.

3. PRACTICAL PROCEDURE

a) Preliminaries: Dilation angle and mean stress

To use the proposed approach and the developed design charts, it is necessary to find an "average" or more precisely, "equivalent" value of the dilation angle of the sand. As both the dilation angle as well as the peak friction angle are functions of the stress level and the packing, they differ from point to point in a soil mass experiencing plastic shearing. In the context of this study, the term "peak friction angle" refers to the maximum friction angle which can be mobilized under a certain stress level. The dilation angle is defined as the ratio of the volumetric strain rate to the maximum shear strain rate, according to Bolton (1986) [28]; it is worth mentioning that the critical state friction angle, $\phi_{c.s.}$, refers to internal frictional angle at zero volumetric strain rate.

Although it is possible to compute the stress level at all points within the domain of the problem (e.g. according to Veiskarami, 2010 [35]), this is often very complicated. More practically, it is possible to assume an average of the stress level acting along the failure surface giving rise to mobilization of the

dilation angle. In this regard, empirical equations by Meyerhof [29] or De Beer [30] can be used, which assumed that the mean (equivalent) stress level, σ_M,is a function of the ultimate pressure beneath the footing, i.e., the bearing capacity,q_{ult}, itself. For example, Meyerhof [29] suggested using 10% of the ultimate pressure whereas De Beer [30] suggested the following expression for the mean stress acting on the failure surface:

$$\sigma_M = 0.25 q_{ult}(1 - \sin\phi) \tag{9}$$

Although these two values do not differ very appreciably, this latter expression was found to be more appropriate according to analyzed cases. Therefore, the equation suggested by De Beer [30] was implemented to establish the procedure.

According to Bolton (1986) [28], both the dilation angle, ψ, and the peak friction angle, ϕ_p,can be related to the critical state friction angle, $\phi_{c.s.}$ and the density index of the sand, D_r. The density index and the critical state friction angle can be measured with better accuracy in the lab and they do not change appreciably with the stress level. Therefore, it appears to be more logical to determine the peak friction and dilation angles based on $\phi_{c.s.}$ and D_r and also the stress level as follows [28]:

$$\phi_p = \phi_{c.s.} + 0.8\psi \tag{10a}$$

$$\phi_p = \phi_{c.s.} + 5I_R \text{ (for plane strain)} \tag{10b}$$

$$\phi_p = \phi_{c.s.} + 3I_R \text{ (for triaxial)} \tag{10c}$$

$$I_R = D_r(Q - \ln\sigma_M) - R \tag{10d}$$

In these equations, the two constants Q and R can be taken equal to 10 and 1 respectively.

b) Explanation of the practical procedure

Since the mean stress level and dilation angle are both unknown at the beginning, an iterative procedure will be required to use the developed design charts for non-associative sands. The iteration comprises the following simple steps:

(i) Choosing appropriate soil constant parameters, i.e. the unit weight, γ, the density index, D_r, and the critical state friction angle, $\phi_{c.s.}$.

(ii) Finding an initial (approximate) value of the bearing capacity, q_{ult}. It can be found by assuming an associated flow rule based on $\phi_{c.s.}$ or by making use of an initial estimate of the dilation angle, ψ (e.g., taking $\psi = 0$) and an initial value of N_γ (by design charts or Eq. 8).

(iii) Computation of the mean stress, σ_M, according to De Beer (1965) [30] (Eq. 9).

(iv) Computation of the peak friction angle, ϕ_p, and the dilation angle, ψ,(Eqs. 10).

(v) Read appropriate value of N_γ from the design charts (or Eq. 8) by using $\phi_p$and ψ.

(vi) Apply an appropriate shape factor, s_γ, if necessary and calculate q_{ult}.

(vii) Repeating steps (ii) through (vi), if necessary, for convergence.

This iterative procedure was found to converge rapidly (e.g. three to five steps). It was noted that if the initial bearing capacity is estimated by choosing the dilation angle equal to half of the critical state friction angle and the peak friction angle accordingly, the method will converge even more rapidly (sometimes in two or three steps). It is again noteworthy that the practical procedure is applicable only to surface footings on sand where the first and second bearing capacity terms vanish. The procedure can be programmed in a simple computer code or an Excel worksheet to accelerate the computational procedure. To do so, it is possible to use the equations provided for the design charts representing the variation of N_γ with the soil friction angle Eq. (8) with corresponding parameters provided in Table 1). Between any two successive curves, a linear interpolation can be made. The rest is nothing but a simple subroutine obeying

a flowchart of the computational routine. It is noticeable that the critical state friction angle is the main parameter based upon which, the analyses are conducted. Thus, it should be measured and/or estimated with care in the laboratory. Once it has been determined, the proposed procedure can be applied.

c) Influence of footing shape and the shape factor

It is important to note at this point that the kinematic approach of the upper bound limit analysis and the proposed approach are mainly for plane strain conditions, that is, they are applicable to strip foundations. For other types of footings it is necessary to apply a proper shape factor as mentioned in the practical procedure. This choice is important since different authors suggested various shape factors based on different assumptions (as stated by Bowles, 1996 [36]). Possibly the first attempt was made by Terzaghi (1943) [5] who suggested different shape factors for square and circular foundations. For circular footings, the radial differential equations for the stresses were derived by Hencky (1923) [37] and led Meyerhof (1963) [7] to take the role of hoop stresses into account and to find some shape factors. Following De Beer (1965) [30], Brinch Hansen (1970) [8] proposed an empirical shape factor in terms of both dimensions and load inclination factors for rectangular foundations based on plate load tests on sand. The same shape factor was assumed by both Brinch Hansen (1970) [8] and Vesić (1973) [9] for vertical loads. Their shape factors do not differ very appreciably with those of Terzaghi (1943) [5], who suggested the shape factors to be 0.8 for square foundations and 0.6 for circular foundations. These shape factors are often used in practice. For the sake of simplicity and uniformity, shape factors of Terzaghi (1943) [5] have been employed in this research. Using these shape factors, the bearing capacity of surface footings on sand can be computed as follows:

$$q_{ult} = 0.5\gamma B N_\gamma s_\gamma \tag{11}$$

where $s_\gamma = 1.0$ for strip foundations, $s_\gamma = 0.8$ for square foundations and $s_\gamma = 0.6$ for circular foundations.

4. WORKED EXAMPLE USING THE PRACTICAL PROCEDURE

In this part, an example of the practical procedure is presented. Experimental data of a footing load test reported by Briaud and Gibbens [38] is presented. This footing load test was a part of a program in Texas A&M University in 1994 and details were provided by FHwA by Briaud and Gibbens [39]. A rough square footing, 3.0m wide, was tested on medium dense silty fine sand ($\phi_{c.s.} = 35°$, $\gamma = 15.5 kN/m^3$and $D_r = 53\%$) with the third bearing capacity factor $N_\gamma = 2q_{ult}/\gamma B s_\gamma = 97.4$. It is notable that the ultimate pressure corresponding to 10% settlement of the footing was estimated to be $q_{ult} = 1800$kPa. For this footing, by implementation of the practical procedure, the following steps were taken:

Assuming $\phi = 35°$ and taking $\psi = 0$, in the first attempt, the bearing capacity factor, N_γ is found to be 28.5 (using Eq. (8)). The shape factor for square footings is $s_\gamma = 0.8$. Therefore, the bearing capacity can be found as $q_{ult} = 0.5\gamma B N_\gamma s_\gamma = 530.5 kPa$. Using this value of q_{ult}, the mean stress can be calculated as $\sigma_M = 56.5$kPa. Based on this mean stress and the density index of the sand, I_R will be 2.16. $\phi_p = 45.8°$ and $\psi = 13.5°$.

Now, a better estimate of $N_\gamma$which accounts for non-associativity, can be found. According to the corresponding graphs and interpolation, N_γ will be roughly 150.1 (note that ψ/ϕ_p ratio is 0.29). The second attempt with this new estimate of N_γ results in $q_{ult} = 2785$kPa, the mean stress $\sigma_M = 197$kPa, $I_R = 1.50$, $\phi_p = 42.5°$ and $\psi = 9.4°$. By using these new values, another iteration can be performed to better estimate the bearing capacity, i.e. $N_\gamma = 88.8$, $q_{ult} = 1648$kPa, $\sigma_M = 133.7$kPa, $I_R = 1.71$, $\phi_p = 43.5°$ and $\psi = 10.7°$ and so on. Eventually, another round of iteration will result in $N_\gamma = 100$

which differs slightly from the one obtained by experiments (nearly 3.3% overestimation). Table 2, shows the iterative procedure to estimate the final value of N_γ. Note that in this table $N_\gamma = 2q_{ult}/\gamma B s_\gamma$.

Table 2. Worked example of using design charts to compute the bearing capacity of non-associative sand

Rounds	ϕ_p **(Deg.)**	ψ **(Deg.)**	ψ/ϕ_p	N_γ	s_γ	q_{ult} **(kPa)**	σ_M **(kPa)**	I_R	ϕ_p **(Deg.)**	ψ **(Deg.)**
Initial (0)	35.0	0.0	0.00	28.5	0.8	530.5	56.5	2.16	45.8	13.5
1	45.8	13.5	0.29	149.7	0.8	2784.7	197.0	1.50	42.5	9.4
2	42.5	9.4	0.22	88.6	0.8	1648.1	133.7	1.71	43.5	10.7
3	43.5	10.7	0.24	103.6	0.8	1927.4	150.0	1.64	43.2	10.3
4	43.2	10.3	0.24	98.9	0.8	1839.8	145.0	1.66	43.3	10.4
5	43.3	10.4	0.24	100.3	0.8	1865.3	146.4	1.66	43.3	10.4
6	43.3	10.4	0.24	99.9	0.8	1857.7	146.0	1.66	43.3	10.4
7	43.3	10.4	0.24	100.0	0.8	1860.0	146.1	1.66	43.3	10.4
8	43.3	10.4	0.24	100.0	0.8	1859.3	146.1	1.66	43.3	10.4
9	43.3	10.4	0.24	100.0	0.8	1859.5	146.1	1.66	43.3	10.4
10	43.3	10.4	0.24	100.0	0.8	1859.5	146.1	1.66	43.3	10.4

At this point, a fundamental question may arise, that is, whether the pivotal parameters of the soil are also converged to the experimental values when the ultimate pressure converged to some value. To further examine this, the database of Briaud and Gibbens [38] and Clark [19] have been revisited. These two cases contain the results of laboratory shear tests. In the first case (according to FHwA, [39]) the angle of dilation is hardly over 2 degrees whereas the converged value is nearly 10 degrees (according to Table 2). The error may be related to the difference between the test condition (under axi-symmetric condition) and the bearing capacity analysis (under plane strain condition). In addition, another reason may be attributed to approximations by Bolton's [28] equation and non-homogeneous nature of the soil in the field.

Clark's [19] data also revealed that there is range of dilation angle for the soil tested in the laboratory between less than 8 to over 30 degrees corresponding to very high and very low confining pressures. The computed and converged angle of dilation was nearly 23 degrees for a circular footing 1.0m in diameter, which shows much better approximation. Both the footing load tests and shear strength tests conducted by Clark [19] were under controlled laboratory condition and the material was reasonably homogeneous. Therefore, it is not surprising that the converged and measured soil properties as well as the predicted and measured bearing capacities are not significantly different. It is noticeable that in both examples, there is an insignificant error in prediction of the ultimate pressure which was the main goal.

It is important to note that the proposed procedure depends mainly on the determination of the critical state friction angle (which can be often determined more conveniently). Care should be taken to extract soil properties from laboratory tests as the accuracy of the proposed procedure is bonded to the accuracy of the laboratory tests measurement and interpretation.

5. COLLECTED DATABASE

A number of footing load test results were collected from the literature. An attempt was made to choose only those cases for which a complete soil data was reported including (but not limited to) the density index, friction angle (preferably the critical state friction angle), shape and roughness of the footing. The database also contains those results of footing load tests located on the surface underlain by sand. In some very limited cases the soil type was composed of a mixture of sand and silt or clay. A wide range of footing dimensions was selected covering both small size and large scale foundations. The range of

footing dimensions falls between small scale (less than 20mm) to large scale (3m) footings. A number of centrifuge tests were also collected which correspond to small to large scale foundations, i.e. up to 10m wide foundations. Thus, a wide range of footing dimensions is covered. Moreover, the range of density indices is between 20% (corresponding to loose sand) and 99% (corresponding to very dense sand). The range of critical state friction angles falls between $26°$and $42°$. Therefore, a rather wide range of footings of different size tested on different sands is covered by the recompiled database. Table 3 shows the collected and recompiled database of footing load tests comprising a total number of 87 case studies. Only the third bearing capacity factor, N_γ, is focused on as it is the only term for shallow footings on sand.

In the first and second columns of this table, the main reference and the soil type are presented. The third column presents the case number. In column (4) the footing shape is presented. The footing shapes were denoted by St (for strip), Sq (for square) and C (for circular). Column (5) presents the ultimate pressure, q_{ult}, where reported in the main reference. Column (6) represents the foundation width, B. Column (7) presents the reported soil friction angle. The soil friction angle is one of the important factors based on which, the bearing capacity is computed. Different values correspond to different states of the soil, i.e., corresponding to loose or a dense state. The values reported in this column correspond to the critical state friction angle, except those provided by Selig and McKee [40] and also Clark (1998) [19] which are peak values. The practical procedure presented in this paper requires the critical state friction angle to be specified as this parameter can often be more precisely measured. Column (8) presents the critical state friction angle, $\phi_{c.s.}$ which is reported in a number of collected data. In absence of such data, for a few cases it was assumed to be equal to the minimum friction angle reported. These assumed values are denoted by an asterisk (*) in the table. Column (9) represents the soil unit weight, γ. Column (10) presents the density index, D_r. In the reported data by Consoli*et al.* [41] the density index was computed based on available data, i.e. the void ratio of the sand. In the rest of the database, the density index was directly reported. Column (11) presents the footing roughness, which is 0 for smooth base footings and 1 for rough base footings. Column (12) presents the third bearing capacity factor, $N_\gamma^{(1)} = 2q_{ult}/\gamma B s_\gamma$. To maintain the consistency between the results, the unfactored values of N_γ were computed and represented in column (13) as $N_\gamma^{(2)} = s_\gamma N_\gamma = 2q_{ult}/\gamma B$. This unfactored N_γ can be used for comparison and to prevent any confusion in definition of N_γ. It should be remarked that for the reported data of Briaud and Gibbens [38] and Consoli*et al.* [41], only the load-displacement curves were reported. Therefore, N_γ was calculated based on the ultimate pressure corresponding to 10% settlement of the footings.

The peak friction angle, wherever required, should be computed with care where Bolton [28] equation is utilized, as the peak friction angle may take irrational values. The reason is too many high values of N_γ for friction angles over $45°$ and hence, overestimation of the bearing capacity. This is often the case where the density index, D_r, is very high and the footing is very small. According to Bolton [28] and other similar works on sand, the peak friction angle should be limited in order to prevent irrational results. For the collected database it was limited to $50°$ which looks practically acceptable and applied to a few cases denoted by a superscript, L next to N_γ in the table. This limitation is logical since it corresponds to $N_\gamma = 618$ (for a rough base foundation) which is still higher than the maximum reported value in the collected database, i.e. 580 (case No. 51).

This collected database has been used to validate the proposed approach and corresponding design charts as well as the practical procedure based on the proposed approach.

Table 3. Collected database of footing load tests on sand

(1)	(2)	(3)	(4)	(5)	(6)	(7)	(8)	(9)	(10)	(11)	(12)	(13)
Reference No.	**Soil Type**	**No.**	**Shape**	**q_{ult} (kPa)**	**B (m)**	**ϕ (Deg.)**	**$\phi_{c.s.}$ (Deg.)**	**γ (kN/m^3)**	**D_r (%)**	**Roughness 0: Smooth 1: Rough**	**$N_\gamma^{(1)}$**	**$N_\gamma^{(2)}$**
Hansen and Odgaard [42]	Sand-Marine Deposit	1	C	62	0.05	36.5	36.5	17	97.1	0	237	142.2^R
		2	C	92	0.1	36.5		17	97.1	0	177	106.2^R
		3	C	26	0.08	30.9	30.9	13.8	9.4	1	84	50.4
		4	C	38	0.15	30.9		13.8	9.4	1	61	36.6
		5	C	43	0.05	34.2	34.2	15.6	62.9	0	182	109.2
		6	C	52	0.1	34.2		15.6	62.9	0	109	65.4
		7	C	86	0.15	34.2		15.6	62.9	0	123	73.8
		8	C	39	0.05	33.8	33.8	15.4	57.7	0	163	97.8
		9	C	40	0.08	33.8		15.4	57.7	0	114	68.4
		10	C	62	0.1	33.8		15.4	57.7	0	132	79.2
		11	C	82	0.15	33.8		15.4	57.7	0	117	70.2
		12	C	28	0.05	32.3	32.3	14.5	31.3	0	124	74.4
		13	C	26	0.08	32.3		14.5	31.3	0	77	46.2
		14	C	36	0.1	32.3		14.5	31.3	0	83	49.8
		15	C	26	0.1	32.3		14.5	31.3	0	58	34.8
		16	C	38	0.15	32.3		14.5	31.3	0	58	34.8
Hansen and Odgaard [42]	Finer Diluvial Sand	17	C	56	0.03	36.7	36*	15.2	51	1	407	244.2
		18	C	69	0.05	36.7		15.2	51	1	295	177.0
		19	C	103	0.08	36.7		15.2	51	1	299	179.4
		20	C	54	0.03	35.8		14.6	35.6	1	408	244.8
		21	C	63	0.05	35.8		14.6	35.6	1	282	169.2
Selig and Mckee [40]	-	22	C	64	0.06	39.5	33*	17.5	97.3	0	212	127.2^R
		23	C	97	0.09	39.5		17.5	97.3	0	215	129.0^R
		24	Sq	64	0.03	39.5		17.5	97	0	180	144.0^R
		25	Sq	104	0.05	39.5		17.5	97	0	195	156.0^R
		26	Sq	132	0.06	39.5		17.5	97	0	185	148.0^R
Vesić, Cerato, [43, 44]	Chattahoochee River Sand	27	C	17	0.05	35.2	35.2	12.8	20.2	1	80	48.0
		28	C	51	0.05	38.4	38.4	13.9	52.8	1	226	135.6
		29	C	70	0.05	42.5	42.5	14.4	65.9	1	301	180.6
		30	C	214	0.15	42.5		14.4	65.9	1	325	195.0
		31	C	21	0.1	35.2	35.2	12.9	23.4	1	55	33.0
		32	C	90	0.1	38.4	38.4	14.1	58.1	1	212	127.2
		33	C	137	0.1	42.5	42.5	14.5	68.4	1	314	188.4
		34	C	37	0.15	35.2	35.2	13.2	32.7	1	60	36.0
		35	C	133	0.15	38.4	38.4	14.2	60.8	1	205	123.0
		36	C	62	0.2	38.4		13.6	45.6	1	76	45.6
		37	C	290	0.2	42.5	42.5	14.8	74.6	1	328	196.8
		38	C	385	0.2	42.5		14.8	74.6	1	435	261.0
		39	C	546	0.2	45	45	14.8	74.6	1	617	370.2^R
		40	C	233	0.05	45		14.9	78.2	1	965	579.0^R
		41	C	371	0.1	45		14.9	78.2	1	830	498.0^R
		42	C	506	0.15	45		14.9	78.2	1	743	445.8^R
Subrahmanyam, Cerato, [45]([44])	Dry, Uniform River Sand	43	C	77	0.05	42	42	15.89	84.6	1	317	190.2
		44	Sq	52	0.02	42		15.89	85	1	320	256.0
		45	Sq	92	0.02	42		15.89	85	1	380	304.0
		46	Sq	95	0.03	42		15.89	85	1	294	235.2
Asgharzadeh - Fozi, Cerato, [46]([44])	Angular, Uniformly Graded Sand, SM	47	Sq	14	0.03	32	32	13.2	20	1	43	34.4
		48	Sq	72	0.03	42	42	14.8	73	1	192	153.6
		49	Sq	106	0.03	42		15.4	89	1	272	217.6
		50	Sq	103	0.03	42		15.4	89	1	264	211.2
Kimura *et al.* [47]	Toyoura Sand	51	St	3.3	0.03	35	35	15.9	84	1	580	580.0^R
		52	St	253	0.3	35		15.9	84	1	450	450.0^R
		53	St	471	0.6	35		15.9	84	1	350	350.0
		54	St	1199	0.8	35		15.9	84	1	300	300.0
		55	St	2428	1.2	35		15.9	84	1	270	270.0
		56	St	3996	1.6	35		15.9	84	1	250	250.0
Clark [19]	Dense Silica Sand	57	C	309	0.1	41.2	36	15.04	88	1	679	407.4^R
		58	C	918	0.5	39.3		15.04	88	1	406	243.6^R
		59	C	1466	1.0	38.5		15.04	88	1	325	195.0
		60	C	4351	5.0	36.8		15.04	88	1	194	116.4
		61	C	6952	10	36		15.04	88	1	156	93.6
Bolton and Lau [48]	Crushed Silica Sand and Silt	62	C	-	1.42	37.5	37.5	16.5	99	1	930	558.0
		63	C	-	3.0	37.5		16.5	99	1	480.5	288.3
		64	C	-	5.0	37.5		16.5	99	1	378.7	227.2
		65	C	-	5.0	37.5		16.7	99	1	237.6	142.6
University of Guilan (2013) (Data from Nemati Mersa,) [49]	Anzali Sand (uniform sand, D_{50}=0.2mm, SP)	66	C	18	0.057	32.7	32.7 (Direct Shear Test)	14.90	30	0	70.6	42.4
		67	C	38	0.057	32.7		15.51	50	0	143.4	86.0
		68	C	54	0.057	32.7		16.32	70	0	193.7	116.2
		69	C	58	0.057	32.7		17.01	90	0	199.5	119.7^R
		70	St	14	0.04	32.7		14.90	30	0	47.0	58.7
		71	St	32	0.04	32.7		15.51	50	0	103.2	127.4

(1)	(2)	(3)	(4)	(5)	(6)	(7)	(8)	(9)	(10)	(11)	(12)	(13)
Reference No.	**Soil Type**	**No.**	**Shape**	q_{ult} **(kPa)**	B **(m)**	ϕ **(Deg.)**	$\phi_{c.s.}$ **(Deg.)**	γ **(kN/m^3)**	D_r **(%)**	**Roughness 0: Smooth 1: Rough**	$N_\gamma^{(1)}$	$N_\gamma^{(2)}$
		72	St	52	0.04	32.7		16.32	70	0	159.5	199.4
		73	St	58	0.04	32.7		17.01	90	0	170.6	213.2[R]
Briaud and Gibbens, Briuad, [38, 50]	Medium dense silty fine sand, SM	74	Sq	1380	1.0	35	35	15.5	53	1	-	178.6
		75	Sq	1500	1.5	35		15.5	53	1	-	130.0
		76	Sq	1580	2.5	35		15.5	53	1	-	81.8
		77	Sq	1600	3.0	35		15.5	53	1	-	68.8
		78	Sq	1800	3.0	35		15.5	53	1	-	77.9
Consoli *et al.* [41]	Medium to fine sand (44%) with silt (32%) and clay (24%)	79	C	300	0.30	26	26	18	42**	1	-	66.7
		80	C	270	0.45	26		18	42**	1	-	40.0
		81	C	240	0.60	26		18	42**	1	-	26.7
		82	Sq	220	0.70	26		18	42**	1	-	27.9
		83	Sq	190	0.40	26		18	42**	1	-	16.9
		84	Sq	280	1.0	26		18	42**	1	-	62.2
Okamura *et al.* (1997), (Yamamoto *et al.*,)[51]	Toyoura Sand D_{50}=0.16-0.2mm	85	C	-	1.5	31	31	9.74	88	0	150	90.0
		86	C	-	2	31		9.74	88	0	139	83.4
		87	C	-	3	31		9.74	88	0	132	79.2

6. ANALYSIS AND VERIFICATION

A number of analyses were made to examine the accuracy of predictions made by the practical procedure based on the proposed approach. As stated earlier, there are limited studies in the literature considering the effect of flow rule. Figure 3 shows a comparison between predictions made by the practical procedure for the collected footing load test database from the literature. It is obvious that the results of the current study are scattered in a narrow band along the 1:1 line indicating reasonably accurate predictions.

The comparisons reveal that reasonable estimates can be obtained if the effect of flow rule is taken into account. To further investigate the accuracy of the practical procedure, one can define a dimensionless bearing capacity ratio, $R_b = N_{\gamma-Computed}/N_{\gamma-Literature}$ where $R_b < 1$ indicates an underestimation and $R_b > 1$ corresponds to overestimation of the bearing capacity. This factor falls between 0.8 and 1.2 corresponding to less than 20% error in prediction of the bearing capacity which is reasonable for practical purpose. The frequency of R_b is presented in Table 4, indicating that in nearly 59.7% of predictions, the predicted value was observed to fall within the range of 0.8 and 1.2, indicating a reasonably good estimate of the bearing capacity. 27.7% of predictions were observed to be underestimated, i.e. in the safe side. Only 12.6% of observations were overestimated values. Therefore, nearly 87% of all observations can be regarded as nearly accurate or at least, in the safe side. As a consequence, the practical procedure seems to be practically applicable to most sands to arrive at a rather accurate, or at least a "safe" estimate of the bearing capacity. Such improved predictions can be related to more realist material strength and failure mechanism in the proposed approach.

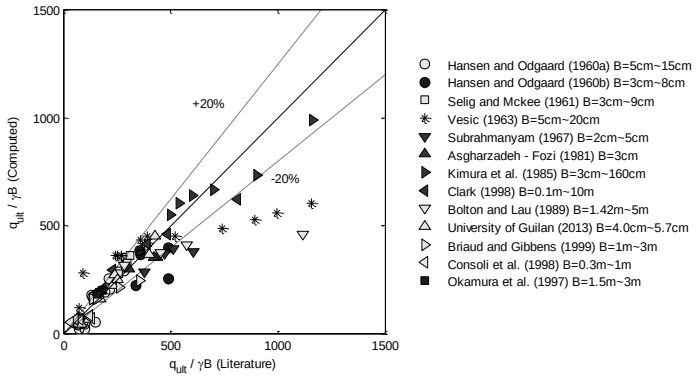

Fig. 3. Bearing capacity factor, $q_{\rm ult}/\gamma B$, computed values by the practical procedure versus reported values in the literature (B: 20mm to10m; $\phi_{\rm c.s.}$: 26 to 42°; D_r: 20% to 99%)

Table 4. Percentage of predictions by the practical procedure in different ranges

Range	Underestimation (Safe Prediction) $R_b < 0.8$	Reasonable Prediction $0.8 < R_b < 1.2$	Overestimation (Unsafe Prediction) $R_b < 1.2$
Percentage of Observations	27.7%	59.7%	12.6%

Errors in estimation of the bearing capacity of sand are still significant, despite the quite careful laboratory tests, measurements and uniformity of the soil. Sources of such errors can be attributed to the method of the analysis, the role of strains and deformation, the footing shape, the footing-soil interface resistance, distribution of the friction angle and the dilation angle throughout the soil body and even, approximations by Bolton's [28] equation. In addition, the interpretation of the ultimate load is also very important, different researchers may use different methods to interpret the ultimate load where there is no apparent peak value) corresponding to the bearing capacity. One can refer to Fellenius [2] for a review of this matter. Observations indicate that the mobilized angle of dilation falls within the range of $0.2\phi_p$to $0.7\phi_p$. Although this range is not always the case when the bearing capacity is analyzed, at least as a rough estimate, it is possible to assume the dilation angle to be $0.4\phi_p$in absence of any accurate experimental data. However such a suggestion is based on the results obtained in this study with all limitations involved in the number of cases and assumptions. Care should be taken to choose appropriate soil parameters for an appropriate prediction of the bearing capacity of sands.

7. CONCLUSION

Following the recent work of the authors in development of a theoretical approach (based on a new kinematic approach of the upper bound limit analysis) to compute the bearing capacity of sand considering the influence of flow rule, the current work is devoted to presenting a practical procedure to estimate the bearing capacity of sands and to examine the accuracy of the proposed approach. While the theory was to some extent well established in the former work of the authors, in the present study, the main focus is on the practical application of the proposed approach. The practical procedure is mainly an iterative procedure in which the bearing capacity factor, N_γ, is computed for non-associative sands. In fact, this procedure employs the results of the proposed approach, i.e. the developed design charts and incorporates equations which related the dilation angle to the mean stress, footing size, state of the sand (expressed in terms of the density index, D_r) and the critical state friction angle, $\phi_{c.s.}$. Since the proposed approach based on a new kinematic approach of the limit analysis has been established for plane strain problems, circular and square foundations require a proper choice of the shape factor. For the sake of simplicity, shape factors of Terzaghi (1943) [5] were adopted for the practical procedure of this research. An example of such iterative procedure was presented.

Verifications were made against a large number of footing load test results found in the literature. The database was collected with care to include all necessary properties of the soil in the test and to cover a wide range of footings and a variety of sands of different density index and friction angle. Results of the analyzed cases revealed that the proposed approach can be reasonably applied to predict the bearing capacity of sands and most of the results are within a reasonable range, or at least, in the safe side.

REFERENCES

1. Fellenius, B. H. (2011). Capacity versus deformation analysis for design of footings and piled foundations. *Geotechnical Engineering Journal of the SEAGS and AGSSEA*, Vol. 42, No. 2, pp. 70-77.
2. Fellenius, B. H. (2015). *Basics of foundation design*. Electronic Edition, (www.fellenius.net).

3. Prandtl, L. (1920). Über die härteplastischerkörper. (About the hardening plastic body), *Nachr.Ges. Wissensch. Göttingen. Math.-Phys. Klasse*, pp. 74–85.
4. Reissner, H. (1924). Zumerddruck problem. *Proc., 1st Int. Congress of Applied Mechanics*, Edited by: C. B. Biezeno and J. M. Burgers, Delft, The Netherlands, pp. 295–311.
5. Terzaghi, K. (1943). *Theoretical soil mechanics*. John-Wiley and Sons Inc., NY.
6. Meyerhof, G. G. (1951). The ultimate bearing capacity of foundations. *Géotechnique*, Vol. 2, No. 4, pp. 301–332.
7. Meyerhof, G. G. (1963). Some recent research on the bearing capacity of foundations. *Can. Geotech. J*., Vol. 1, pp. 16–26.
8. Brinch Hansen, J. (1970). A revised and extended formula for bearing capacity. *Danish Geotechnical Institute Bulletin*, Vol. 28, pp. 5–11.
9. Vesić, A. S. (1973). Analysis of ultimate loads of shallow foundations. *J. Soil Mech. Found. Div.*, ASCE, Vol. 99, pp. 45–73.
10. Sokolovskii, V. V. (1960). *Statics of granular media*. (translatedby J. K. Lusher and edited by A. W. T. Daniel), Pergamon Press, London.
11. Drucker, D. C. & Prager, W. (1952). Soil mechanics and plastic analysis on limit design. *Quart. Appl. Math.*, Vol. 10, pp. 157–165.
12. Bottero, A., Negre, R., Pastor, J. & Turgman, S. (1980). Finite element method and limit analysis theory for soil mechanics problems. *Computer Methods in Applied Mechanics and Engineering*, Vol. 22, pp. 131-149.
13. Sabzevari, A. & Ghahramani, A. (1972). The limit equilibrium analysis of bearing capacity and earth pressure problems in nonhomogeneous soils. *Soils Found.*, Vol. 12, No. 3, pp. 33–48.
14. Bolton, M. D. & Lau, C. K. (1993). Vertical bearing capacity factors for circular and strip footings on Mohr-Coulomb soil. *Can. Geotech. J.*, Vol. 30, pp. 1024–1033. (DOI: 10.1139/T93-099).
15. Kumar, J. (2003). $N_{\square}$ for rough strip footing using the method of characteristics. *Can. Geotech. J.*, Vol. 40, No. 3, pp. 669–674. (DOI: 10.1139/T03-009).
16. Martin, C. M. (2005). Exact bearing capacity calculations using the method of characteristics. *Proc. 11th Int. Conf. of IACMAG*, Vol. 4, Turin, pp. 441–450.
17. Jahanandish, M., Habibagahi, G. & Veiskarami, M. (2010a). Bearing capacity factor, $N_{\square}$, for unsaturated soils by ZEL method. *ActaGeotechnica*, Springer, No. 5, 177–188. (DOI: 10.1007/s11440-010-0122-3).
18. Kumar, J. (2009). The variation of N_{γ} with footing roughness using the method of characteristics. *Int. J. Numer. Anal. Meth. Geomech.* Vol. 33, 275–284. (DOI: 10.1002/nag.716).
19. Clark, J. I. (1998). The settlement and bearing capacity of very large foundations on strong soils. 1996 R.M. Hardy Keynote address, *Can. Geotech. J.*, Vol. 35, pp. 131–145.
20. Zhu, F., Clark, J. I. & Phillips, R. (2001). Scale effect of strip and circular footings resting on dense sand. *J. Geotech. Geoenviron. Eng.*, ASCE, Vol. 127, No. 7, pp. 613–621.
21. Cerato, A. B. & Lutenegger, A. J. (2007). Scale effects of shallow foundation bearing capacity on granular material. *J. Geotech. Geoenviron. Eng.*, ASCE, Vol. 133, No. 10), pp. 1192–1202. (DOI: 10.1061/(ASCE)1090-0241(2007)133:10(1192)).
22. Jahanandish, M., Veiskarami, M. & Ghahramani, A. (2010b). Effect of stress level on the bearing capacity factor, $N_{\square}$, by the ZEL method. *KSCE Journal of Civil Engineering*, Springer, Vol. 14, No. 5, pp. 709-723.
23. Michalowski, R. L. (1997). An estimate of the influence of the soil weight on the bearing capacity using limit analysis. *Soils Found.*, Vol. 37, No. 4, pp. 57–64.
24. Frydman, S. & Burd, H. J. (1997). Numerical studies of the bearing capacity factor, $N_{\square}$.. *J. Geotech. Geoenviron. Eng.*, ASCE, Vol. 123, No. 1, pp. 20–29.

25. Yin, J. H., Wang, Y. J. & Selvadurai, A. P. S. (2001). Influence of non-associativity on the bearing capacity of a strip footing. *J. Geotech. Geoenviron. Eng.*, ASCE, Vol. 127, No. 11, pp. 985–989.
26. Jahanandish, M. (2003). Development of a Zero Extension Line method for axially symmetric problems in soil mechanics. *ScientiaIranica*, Sharif University of Technology, Vol. 10, No. 2, pp. 203-210.
27. Veiskarami**,** M., Kumar, J. & Valikhah, F. (2014). Effect of flow rule on the bearing capacity of strip foundations on sand by the upper bound limit analysis and slip lines. *Int. J. Geomech*., ASCE, Vol. 14, No. 3, 04014008 1-14. DOI: 10.1061/(ASCE)GM.1943-5622.0000324.
28. Bolton, M. D. (1986). The strength and dilatancy of sands. *Géotechnique*, Vol. 36, No. 1, pp. 65–78. (DOI: 10.1680/geot.1986.36.1.65).
29. Meyerhof, G. G. (1950). *The bearing capacity of sand* .Ph.D. Dissertation, Univ. of London.
30. De Beer, E. E. (1965). Bearing capacity and settlement of shallow foundations on sand. *Proc. of the Bearing Capacity and Settlement of Foundations Symposium*, Duke University, Durham, N. C., pp. 15–34.
31. Chen, W. F. & Liu, W. (1990). *Limit analysis in soil mechanics*. Elsevier.
32. Harr, M. E. (1966). Foundations of theoretical soil mechanics. McGraw-Hill.
33. Keshavarz, A., Jahanandish, M. & Ghahramani, A. (2011). Seismic bearing capacity analysis of reinforced soils by the method of stress characteristics. *Iranian Journal of Science and Technology, Transaction B: Engineering*, Shiraz University, Vol. 35, No. C2, pp. 185-197.
34. Kötter, F. (1903). *Die bestimmung des druckesangekrümmtengleitflächen, eineaufgabeaus der lehrevomerddruck*. Sitzungsberichte der akademie der wissenschaften, Berlin, pp. 229–233.
35. Veiskarami, M. (2010). Stress level based prediction of load-displacement behavior and bearing capacity of foundations by ZEL method. Ph.D. Dissertation, Shiraz University, May 2010, Shiraz, Iran.
36. Bowles, J. E. (1996). *Foundations analysis and design*. 5th ed. McGraw- Hill, New York.
37. Hencky, H. (1923). Übereinigestatischbestimmte Falle des Gleichgewichts in plastischenKorpern. Z. Angew. Math. Mech.
38. Briaud, J. L. & Gibbens, R. M. (1999). Behavior of five large spread footings in sand. *J. Geotech. Geoenviron. Eng.*, ASCE, Vol. 125, No. 9, pp. 787-796.
39. FHwA (1997). Large-scale load tests and database of spread footings on sand. Publication Number FHWA-RD-97-068, Nov. 1997, by Jean-Louis Briaud and Robert Gibbens.
40. Selig, E. T. & McKee, K. E. (1961). Static and dynamic behavior of small footings. *J. Soil Mech. Found. Div.*, ASCE, Vol. 87, pp. 29–47.
41. Consoli, N. C., Schnaid, F. & Milititsky, J. (1998). Interpretation ofplate load tests on residual soil site. *J. Geotech. Geoenviron. Eng.*, Vol. 124, No. 9, pp. 857–867.
42. Hansen, B. & Odgaard, D. (1960). Bearing capacity tests on circular plates on sand. *The Danish Geotechnical Institute*: Bulletin No. 8.
43. Vesić, A. S. (1963). Bearing capacity of deep foundations in sand. Highway Research Record No. 39, Highway Research Board (HRB), pp. 112-153.
44. Cerato, A. B. (2005). Scale effect of shallow foundation bearing capacity on granular material. Ph.D. Dissertation, University of Massachusetts Amherst, USA.
45. Subrahmanyam, G. (1967). The effect of roughness of footings on bearing capacity. *J. I.N.S. Soil Mech. Found. Eng.* Vol. 6, pp. 33–45.
46. Asgharzadeh-Fozi, Z. (1981). Behavior of square footing on reinforced sand. M.Sc. Thesis, San Diego State University.
47. Kimura, T., Kusakabe, O. & Saitoh, K. (1985). Geotechnical model tests of bearing capacity problems in a centrifuge. *Géotechnique*, Vol. 35, No. 1, pp. 33–45.

48. Bolton, M. D. & Lau, C. K. (1989). Scale effect in the bearing capacity of granular soils. *Proc. 12th Int. Conf. Soil Mech. Found. Eng.*, Rio De Janeiro, Brazil, Vol. 2, 895-898.
49. NematiMersa, A. (2013). Numerical and Experimental Analysis of the Post-Liquefied Anzali Sand Bearing Capacity by Glass Tank Apparatus, M.Sc. Thesis, University of Guilan, March 2013, Guilan, Iran.
50. Briaud, J. L. (2007). Spread footings in sand: Load settlement curve approach. *J. Geotech. Geoenviron. Eng.*, ASCE, Vol. 133, No. 8, pp. 905-920. (DOI: 10.1061/(ASCE)1090-0241(2007)133:8(905)).
51. Yamamoto, N., Randolph, M. F. & Einav, I. (2009). Numerical study of the effectof foundation size for a wide range of sands. *J. Geotech. Geoenviron. Eng.*, ASCE, Vol. 135, No. 1, pp. 37–45. (DOI: 10.1061/(ASCE)1090-0241(2009)135:1(37)).